Inorganic Chemistry

Article

pubs.acs.org/IC

Interaction between Proteins and Ir Based CO Releasing Molecules: Mechanism of Adduct Formation and CO Release

Ariel A. Petruk,[†] Alessandro Vergara,[‡,§] Daniela Marasco,[§,∥] Damian Bikiel,[†] Fabio Doctorovich,[†] Dario A. Estrin,[†] and Antonello Merlino*[,‡,§]

[†]Departamento de Química Inorgánica, Analítica y Química Física/INQUIMAE-CONICET, University of Buenos Aires, Ciudad Universitaria, Pab. 2, C1428EHA Buenos Aires, Argentina

[‡]Department of Chemical Sciences, University of Naples Federico II, via Cintia I-80126, Napoli, Italy

[§]CNR Institute of Biostructures and Bioimages, Via Mezzocannone 16 I-80100, Napoli, Italy

[∥]Department of Pharmacy, CIRPEB: Centro Interuniversitario di Ricerca sui Peptidi Bioattivi- University of Naples Federico II, DFM-Scarl, Via Mezzocannone, 16 80134, Napoli, Italy

Supporting Information

ABSTRACT: Carbon monoxide releasing molecules (CORMs) have important bactericidal, anti-inflammatory, neuroprotective, and antiapoptotic effects and can be used as tools for CO physiology experiments, including studies on vasodilation. In this context, a new class of CO releasing molecules, based on pentachlorocarbonyliridate(III) derivative have been recently reported. Although there is a growing interest in the characterization of protein−CORMs interactions, only limited structural information on CORM binding to protein and CO release has been available to date. Here, we report six different crystal structures describing events ranging from CORM entrance into the protein crystal up to the CO release and a biophysical characterization by isothermal titration calorimetry, Raman microspectroscopy, and molecular dynamics simulations of the complex between a pentachlorocarbonyliridate(III) derivative and hen egg white lysozyme, a model protein. Altogether, the data indicate the formation of a complex in which the ligand can bind to different sites of the protein surface and provide clues on the mechanism of adduct formation and CO release.

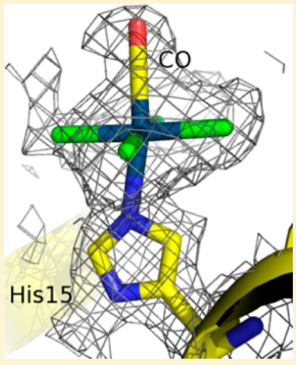

INTRODUCTION

Carbon monoxide (CO) is a colorless, odorless stable gas that occurs in nature as a product of oxidation or combustion of organic matter. Owing to its lethal effect when present at high concentrations, CO was considered for many years to be only a toxic molecule that results from air pollution by car exhaust. The discovery that CO is also a product of heme metabolism by heme oxygenases and that it can interact effectively with disparate targets, such as soluble guanylate cyclase, cytochrome c oxidase, NADPH oxidase, or potassium channels to transduce important signals within cells, has modified our perception of CO as an environmental toxicant and has opened a new area of investigation on the biological properties of this molecule. Important results in this field have been obtained using CO releasing molecules (CORMs), a group of compounds capable of delivering defined amounts of CO into cellular systems, thereby reproducing the biological effects of CO derived from hemeoxygenase activity.[1−3] These molecules represent a useful pharmacological tool to exploit the bioactive properties of CO minimizing its toxicity. CORMs have been developed for the treatment of fibrosis, inflammation, cancer, or other pathologic states associated with excessive protein synthesis or hyperproliferation.[4] In fact, they have bactericidal,[5] anti-inflammatory,[6,7] antiapoptotic,[8] antimicrobial,[9] and antiproliferative effects[10] in many cell types. Furthermore, they show neurotherapeutic and neurometabolic effects.[11] The first generation of CORMs involved complexes of Mn and Fe, like $[Mn_2(CO)_{10}]$ and $Fe(CO)_5$,[3] and of Co,[12] and their photoreaction in water have been recently studied.[13] Further developments led to ruthenium derivatives, for example $[Ru(CO)_3Cl_2]_2$ and tricarbonylchloro(glycinato) ruthenium-(II) $[RuCl(gly)(CO)_3]$, named CORM-3.[5] In this context, an interesting class of new CORMs based on $[IrCl_5CO]^{2-}$ derivatives has been very recently developed.[14] These compounds are soluble in aqueous media, are able to release CO spontaneously (i.e., without irradiation by light), and present CO-releasing rates comparable with those observed for known CORMs.[14] In spite of the increasing expectations for the use of CORMs in medicine, until now, very little is known about the possible interactions of these molecules with proteins[15] and even less about the successive CO release. A review on the elucidated crystal structures of organometallic-protein complexes, including CO containing metallodrugs, has been very recently reported by Herrick, Ziegler, and Leeper.[16]

In a recent paper the crystal structure of hen egg white lysozyme (HEWL) complexed with CORM-3 at 1.5 Å resolution has been reported.[17] The interaction of other Ru-

Received: June 27, 2014
Published: September 12, 2014

   dx.doi.org/10.1021/ic501498g | *Inorg. Chem.* 2014, 53, 10456−10462

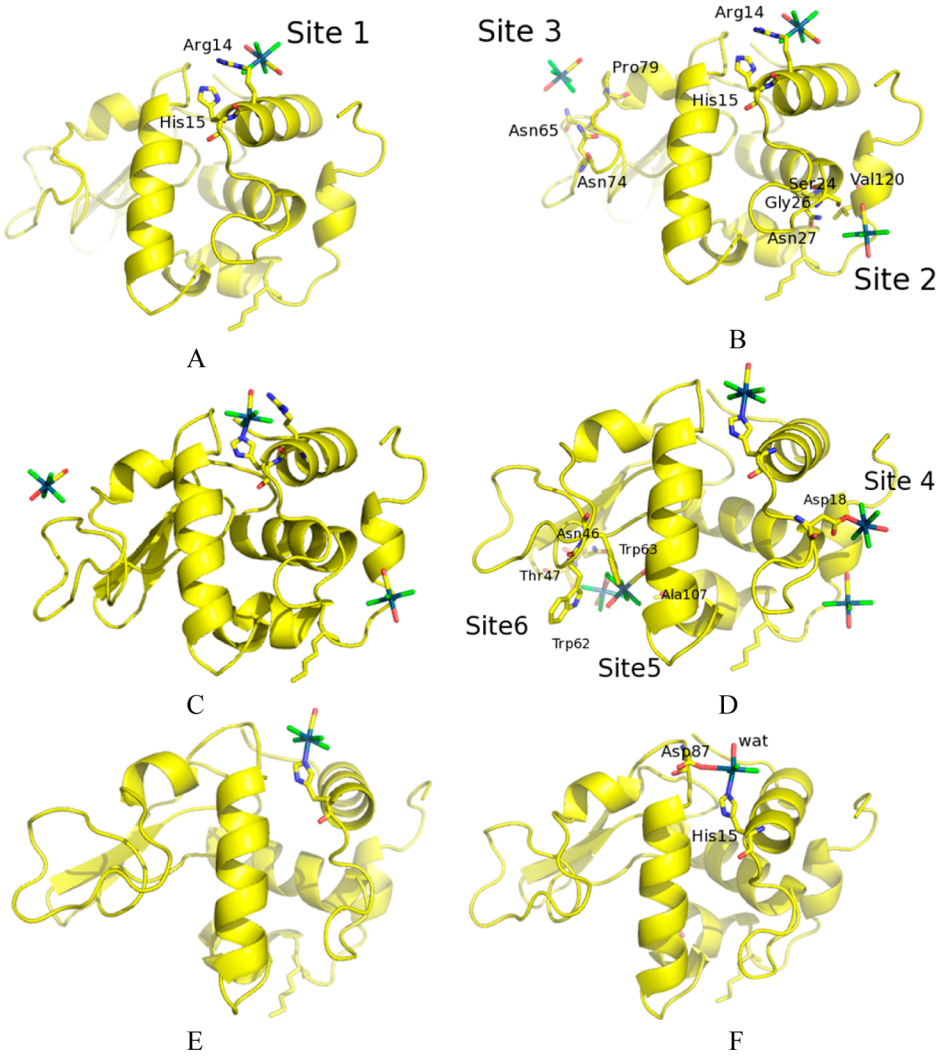

Figure 1. Overall structures of HEWL bound to $[IrCl_5CO]^{2-}$ moieties. The structures have been refined using data collected on crystals exposed to $[IrCl_5CO]^{2-}$ at different times (1 day (A), 4 days (B), 5 days (C), 6 days (D), 9 days (E), and 30 days (F)). The occupancy factor of iridium complex ranges from 0.29 to 1.0. In particular, the highest occupancy value for each site is 1.00, 1.00, 0.52, 0.70, 0.39, and 0.29 for the site from 1 to 6, respectively. C atoms are colored in yellow, oxygens are in red, nitrogen are in blue, iridium is in light blue, and Cl is in green.

containing CORMs with HEWL has been also studied.[17−20] Binding sites have been envisaged in diverse locations, i.e. close to His15, Asp18, Asp101, and Asp119.[19] Here we report a crystallographic and molecular dynamics study on the binding mode of $[IrCl_5CO]^{2-}$ to HEWL. The results herein presented provide the first high-resolution crystal structures for a CO-containing iridium derivative−protein adduct, and more significantly, they shed light on the CO release process.

EXPERIMENTAL SECTION

Materials. Hen egg white lysozyme (HEWL), sodium chloride, sodium acetate, acetic acid, and $K_3[IrCl_6]$ was purchased from Sigma−Aldrich. $Cs_2[IrCl_5CO]$ was prepared starting from $[IrCl_6]^{3-}$ as previously reported.[14]

Crystallization and Data Collection. HEWL was crystallized using the hanging drop vapor diffusion method and 1.2 M NaCl as a precipitating agent in 0.050 M acetate buffer pH 4.5. Crystals of 0.2−0.5 mm size appeared within 12−24 h and were stabilized overnight with a harvesting solution containing 1.4 M NaCl in the same buffer. A saturated solution of $Cs_2[IrCl_5CO]$ was prepared in harvesting buffer and added to the crystal drops. Yellow protein crystals were flash frozen at 100 K, using the dehydration process,[21] after 20 min, 4 h, and 1, 4, 5, 6, 9, and 30 days of storage at 25 °C in a temperature-controlled room, where they are sporadically exposed to visible light. The dehydration process removes the need for cryoprotectants to be used, ruling out any effect that the cryoprotectants might have had on binding to the protein.[21] A complete data set was collected for all these crystals, but analysis of the Fo-Fc electron density maps obtained using the first two data collections (i.e., after 20 min and 4 h) does not show evidence of Ir complexes bound to HEWL. Data sets were collected at the Institute of Biostructure and Bioimages of CNR, Naples, Italy on a Saturn944 CCD detector using Cu Kα radiation from a Rigaku Micromax 007 HF generator. Data were indexed and scaled using HKL2000.[22] All the crystals belonged to $P4_32_12$ space group and diffracted at high resolution (1.44−1.99 Å). In almost all cases, overall completeness of data is close to 100%, R_{merge} is <0.116.

Structure Refinement. The structures were solved with rigid body refinement using CNS1.3[23] and coordinates of the PDB entry 193L.[24] Several cycles of restrained refinement followed by visual inspection, model building, adjustment in O[25] were performed in order to improve the models. The iridium peak positions were identified using anomalous difference electron-density maps as a cross-check with Fo - Fc electron-density maps. $[IrCl_4CO(H_2O)]^-$ moieties, i.e. the product of the hydrolysis of $[IrCl_5CO]^{2-}$, were manually fitted in the electron density maps. Structure validation was carried out using Procheck[26] and Whatcheck.[27] The coordinates and structure factor have been deposited in PDB with accession codes 4n9r, 4nhp, 4nhq,

dx.doi.org/10.1021/ic501498g | Inorg. Chem. 2014, 53, 10456−10462

4nht, 4nhs, and 4nij. Refinement statistics were reported in Table S1 in the Supporting Information.

Raman Microscopy. Raman microspectroscopy data were collected at the Department of Chemical Sciences of University of Naples Federico II, using an apparatus described elsewhere.[28] Raman spectra were collected for HEWL crystals, $Cs_2[IrCl_5CO]$ powder and for HEWL crystals soaked in a saturated solution of $Cs_2[IrCl_5CO]$ in 1.2 M NaCl, 0.050 M sodium acetate pH 4.5. In order to assist the Raman assignment of the medium frequency bands, opening and closure of the crystallization box were also performed in an additional experiment after 1 day of soaking and re-equilibration was followed. The excitation line was 647 nm, with a power at the sample of 2 mW. Spectral resolution was 4 cm^{-1}. These experiments have been performed using crystals that were sporadically exposed to visible light.

Molecular Dynamics Simulations. Molecular dynamics simulations were performed using the coordinates of the crystal structure of HEWL, including the Ir complexes, obtained after 6 days of soaking ("6 days" crystal structure) as starting model. The system was immersed in a box of TIP3P water molecules.[29] The minimum distance between the protein and wall was 10 Å. The system was simulated employing periodic boundary conditions and Ewald sums for treating long-range electrostatic interactions.[30] The shake algorithm was used to keep bonds involving the H atom at their equilibrium length. This allowed us to employ a 2 fs time step for the integration of Newton's equations. The temperature and pressure were regulated with the Berendsen thermostat and barostat, respectively, as implemented in AMBER.[31] The cut off used was 8 Å for the van der Waals interactions. The system was first minimized to optimize any possible structural clashes. Subsequently, the system was heated slowly from 0 to 300 K under constant volume conditions. Finally, a short simulation at a constant temperature of 300 K under a constant pressure of 1 bar was performed, to allow the systems to reach proper density. These equilibrated structures were the starting point for 50 ns of MD simulations. Standard Amber parm99 parameters[32] were used for the protein. For $[IrCl_4CO(H_2O)]^-$ and $[IrCl_4CO(His)]^-$ parametrization, a protocol similar to that used in other protein–metal complexes was implemented.[33] Partial charges were RESP charges computed using DFT method and B3LYP/6-31G* basis set for C, N, O, and H atoms while the LANL2DZ basis set and pseudopotential was used for the Ir atom.[34] RESP charges used for our calculations are reported in Table S2 in the Supporting Information.

Implicit Ligand Sampling Calculation. The free energy maps for the CO migration process inside the protein core were computed by the implicit ligand sampling (ILS) approach[35] that uses MD simulations in the absence of the ligand and incorporate it afterward. Details on this method can be found elsewhere.[36,37] Briefly, in the ILS method, the free energy of placing a ligand in a site on the surface or in buried regions of a protein is computed using a statistical thermodynamic approach and dividing the space in a finite grid. ILS calculations were performed in a rectangular grid (0.5 Å resolution) that includes HEWL; the probe used was a CO molecule. Calculations were performed on 500 frames taken from the 50 ns MD simulation.

RESULTS AND DISCUSSION

Adduct Formation. We present six crystal structures of the complex formed between HEWL and $[IrCl_5CO]^{2-}$ that differ in the incubation time of preformed HEWL crystals with the Ir-compound. The three-dimensional structures of the protein:Ir-compound adduct have been analyzed by difference Fourier techniques. The structures have been deposited in the Protein Data Bank with codes 4n9r, 4nhp, 4nhq, 4nht, 4nhs, and 4nij. Overall structures of HEWL bound to $[IrCl_5CO]^{2-}$ moieties are reported in Figure 1. The inspection of electron density maps of the six structures shows that the complex can bind to the protein at up to six different sites close to His15 (site 1); Ser24, Asn27, and Val120 (site 2); Asn65 and Pro79 (site 3); Asp18 (site 4); Asn59, Trp62, Trp63, and Ala107 (site 5); and Asn46 and Thr47 (site 6). These results agree with ITC data that suggest the presence of multiple Ir-compound binding sites on the protein surface (Figure S1 of the Supporting Information).

The binding did not cause any significant change in the overall protein structure as judged by r.m.s. deviations in the range 0.11–0.25 Å for the superposition of the Cα atoms of native protein with those of the complexes.

The comparison among the structures refined using data collected on crystals exposed to $[IrCl_5CO]^{2-}$ at different times (Figure 1) suggests a plausible mechanism of adduct formation.

In the "1 day" structure, the Ir complex that has exchanged the Cl atom trans to CO with a water molecule from the medium binds to HEWL surface with one Cl (Cl1) interacting with NH atom of Arg14 (Figure 2). The binding of the Ir compound to this site (site 1) is further stabilized by hydrogen bonds that CO forms with water molecules that in turn are hydrogen-bonded to the carbonyl group of Arg128 (Figure 2).

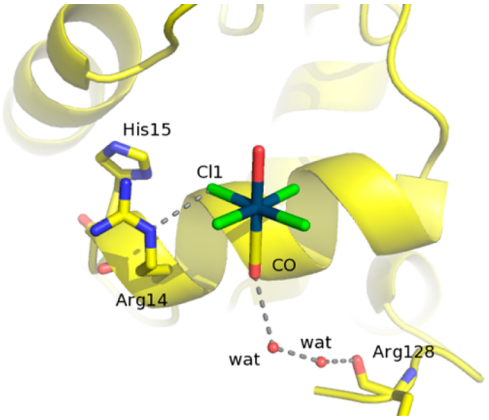

Figure 2. Geometry and coordination of ligand at the site 1 in the "1 day" structure. Hydrogen bonds between the Ir complex and protein residues are depicted in dashed lines.

In the "4 days" structure, two additional sites are found (Figure 1). In the former (site 2), Cl1 and Cl3 atoms are close to ND atom (i.e., the N side chain atom) of Asn27 and N amide atom of Val120, respectively. The CO group is hydrogen-bonded to the OG atom of Ser24 and to a water molecule, which in turn is hydrogen-bonded to the amide N of Gly26 (Figure 3).

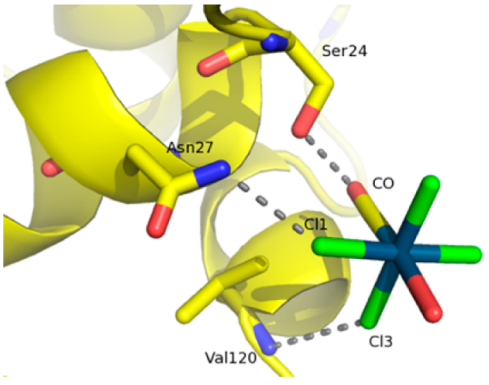

Figure 3. Geometry and coordination of the ligand at the site 2 in the "4 days" structure. Hydrogen bonds between the Ir complex and protein residues are depicted in dashed lines. The water molecule that bridges CO with the N atom of Gly26 is omitted for the sake of clarity.

dx.doi.org/10.1021/ic501498g | Inorg. Chem. 2014, 53, 10456–10462

In the latter (site 3), the complex is bound on the protein surface in a cleft formed by Asn65, Asn74, and Pro79 (Figure 4). Within this site, Cl2 and Cl3 and the water ligand are bound

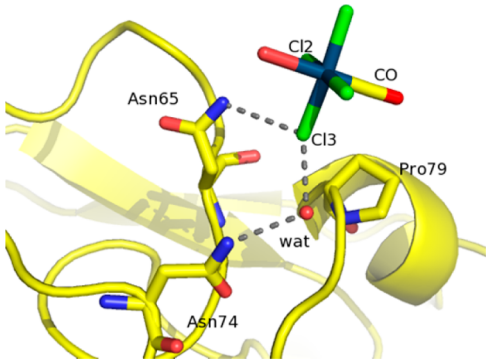

Figure 4. Geometry and coordination of the ligand at the site 3 in the "4 days" structure. Hydrogen bonds between the complex and protein residues are depicted in dashed lines. The interaction between the water ligand and the side chain of Asn65 has been omitted.

to ND side chain atoms of Asn65 and to a water molecule, which is also involved in the formation of hydrogen bonds with the side chain of Asn74.

In the "5 days" structure, the $[IrCl_4CO(H_2O)]^-$ molecule, i.e., the product of $[IrCl_5CO]^{2-}$ hydrolysis in water, coordinates to the protein (Figure 5): upon protein−Ir derivative adduct

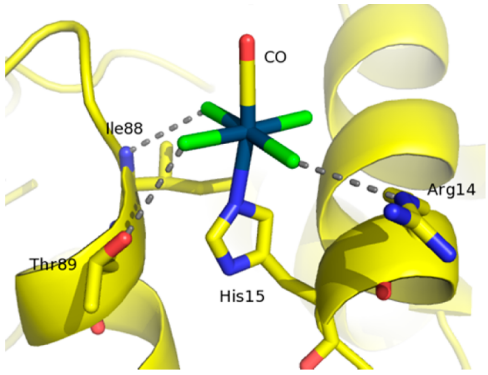

Figure 5. Geometry and coordination of ligand at the site 1 in the "5 days" structure. Hydrogen bonds between the Ir complex and protein residues are depicted in dashed lines.

formation, the water molecule is lost and the vacant coordination position is filled with the side chain of His15. It is possible that a mixture of $[IrCl_4CO(H_2O)]^-$ and the Ir complex bound to His coexist in the crystal. However, in our model, only the adduct with the ligand bound to His15 has been considered. In the adduct, Ir adopts a slightly distorted octahedral geometry with the NE2 of His side chain and the CO molecule occupying the axial positions and the chloride atoms on the equatorial positions. Interestingly, at variance with what was found in the case of CORM-3/HEWL adduct,[17] where Ru binds His15 with occupancy of 0.8 and chlorides are lost in the complex formation, in the present structure the Ir derivative moiety retains both the Cl atoms and the CO, as judged by the analysis of B-factors and by the inspection of anomalous electron density maps (data not shown). Cl1 interacts with NH amide of Ile88, Cl2 with OH side chain atom of Thr89 (Figure 5), and Cl3 with NH side chains groups of Arg14.

In the "6 days" structure, the site 3 becomes unoccupied (Figure 1D), but other three new binding sites emerge (Figures 6 and 7). The first one is close to Asp18 (site 4) (Figure 6). In

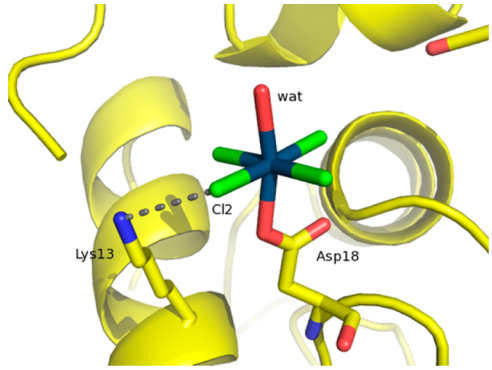

Figure 6. Geometry and coordination of ligand at the site 4 in the "6 days" structure. Hydrogen bonds between the complex and protein residues are depicted in dashed lines.

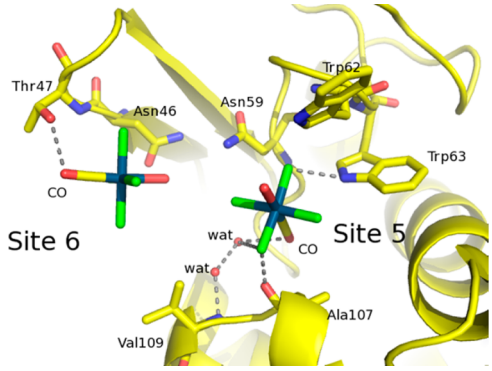

Figure 7. Geometry and coordination of ligand at the sites 5 and 6 in the "6 days" structure. Hydrogen bonds between the complex and protein residues are depicted in dashed lines.

this site, the Ir compound has lost the CO molecule (Figure 6). The second new Ir compound binding site is close to Asn59, Trp62, Trp63, and Ala107 (site 5; Figure 7). The site 6 is close to Asn46 and Thr47 (Figure 7).

In the "9 days" structure, all Ir compounds excluding that bound to site 1 leave the protein surface (Figure 1E). Geometry and coordination of the ligand in this structure is similar to that described for the "5 days" structure.

In the "30 days" structure (Figure 1F), the Ir compound in the site 1 has lost the CO molecule (Figure 8) which is replaced by a water molecule. In this structure, an oxygen atom of the side chain of Asp87 replaces one of the Cl ligands.

Since the experiments have been performed in the presence of visible light, we cannot exclude that a photochemical reaction is involved in the CO-release process.

To check the stability of the above-described HEWL−Ir compound interactions, we have performed a 50 ns molecular dynamics (MD) simulation using the "6 days" structure as starting model. This structure includes the Ir complexes bound to sites 1, 2, 4, 5, and 6. The results of the MD study show that all the Ir-compounds leave the protein surface in the first 5 ns. Ala10, Lys13, Leu25, and Asn93 are the residues which interact for longer times with the Ir derivative (see Figure S2 of the

dx.doi.org/10.1021/ic501498g | Inorg. Chem. 2014, 53, 10456−10462

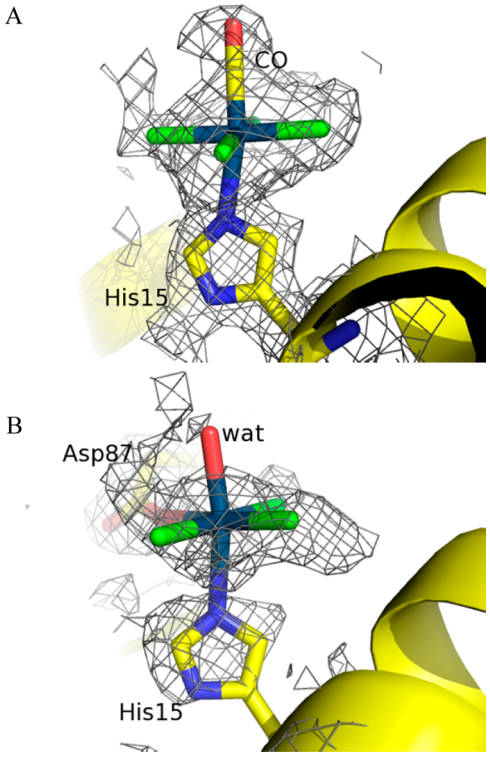

Figure 8. 2Fo-Fc electron density map at 0.8 σ of the site 1 in the "4 days" (A) and "30 days" (B) structure.

Supporting Information for the location of these residues on the HEWL surface). Visual inspection of the simulation frames suggests that the protein–Ir compound interactions are mainly driven by the CO group. This hypothesis has been verified by calculating the correlation between the orientation of the CO toward the protein surface and the formation of stabilizing interactions between the Ir compound and the protein. The correlation value was as high as 0.86.

CO Release. An interesting result of this work is the observation of the CO ligand release from the adduct at longer times (Figures 1 and 8).

In the HEWL-$[IrCl_4CO(H_2O)]^-$ adduct, the CO release process seems associated with the loss of interacting molecules on the HEWL surface (Figure 1E,F), further supporting the idea that the presence of CO on the Ir compound has an important role in the protein–ligand recognition. These results are indirectly supported by the X-ray structure of the complex between HEWL and $[IrCl_6]^{3-}$ showing that this ligand binds to different regions of the HEWL surface when compared to $[IrCl_4CO(H_2O)]^-$ (data not shown).

Vibrational spectroscopy studies of biorelevant metal carbonyl compounds have been often used to characterize the CO-release process.[38−41] Here, examination of changes in the Raman spectra further corroborates the crystallographic data. Raman microspectroscopy was used to monitor the ligand exchange process for Ir ligands, with particular interest in CO release, in HEWL crystals. Reproducible Raman spectra during $[IrCl_5CO]^{2-}$ soaking into HEWL crystals were collected in off-resonance conditions (647 nm line) using a setup elsewhere described.[28] Raman spectra of $Cs_2[IrCl_5CO]$ powder were collected as reference as well.

Spectra were registered both in the low frequency (200–1300 cm^{-1}, Figure 9) and in the medium frequency (1300–2300 cm^{-1}, Figure 10) regions. The major Raman bands in the

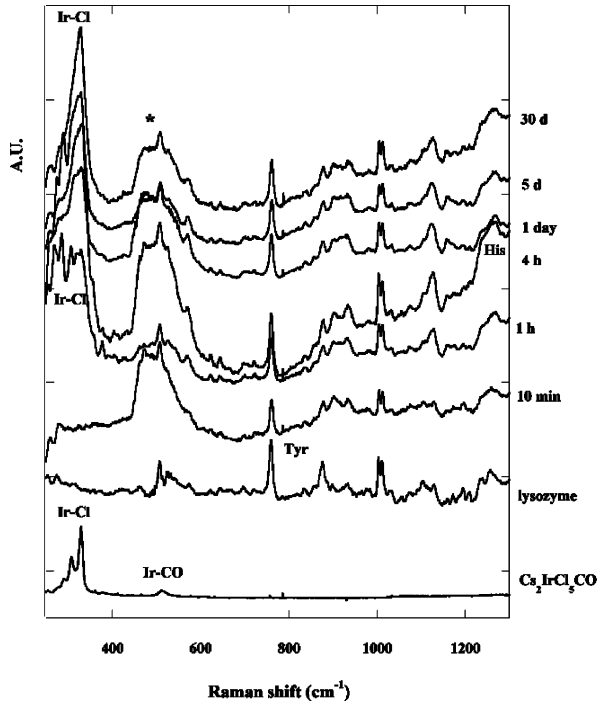

Figure 9. Low frequency Raman spectra of $Cs_2[IrCl_5CO]$ powder, lysozyme crystals and of protein crystals soaked in a saturated solution of $Cs_2[IrCl_5CO]$ as a function of time. Star refers to signals from buffer. Excitation line 647 nm; power at the sample 2 mW; spectral resolution 4 cm^{-1}.

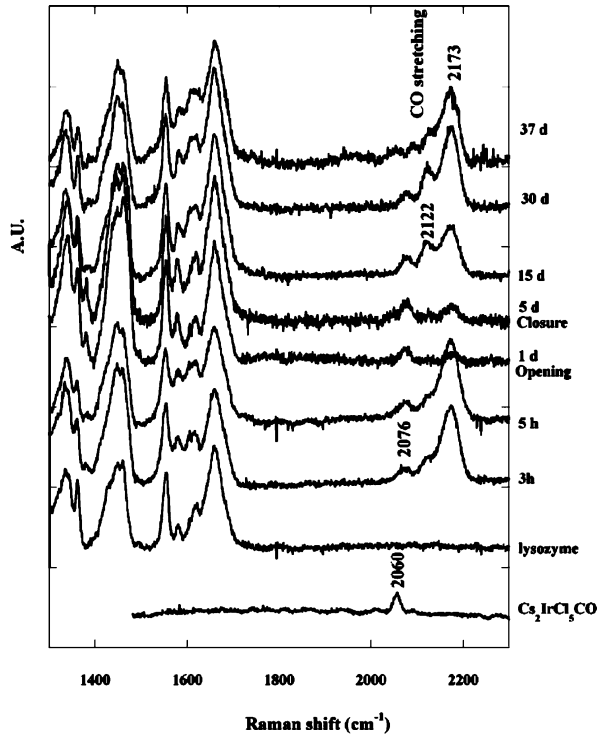

Figure 10. Medium frequency Raman spectra of $Cs_2[IrCl_5CO]$ powder, lysozyme crystals, and protein crystals soaked in a saturated solution of $Cs_2[IrCl_5CO]$ as a function of time. Opening and closure labels refer to the time of opening and closure of the crystallization box (see text for rationale). Excitation line 647 nm, power at the sample 2 mW, spectral resolution 4 cm^{-1}. In this experiment it is possible that a photochemical reaction can assist the CO releasing process.

dx.doi.org/10.1021/ic501498g | Inorg. Chem. 2014, 53, 10456−10462

powder (Ir−Cl and CO stretching) are well visible, though slightly shifted in the aqueous solution/crystal after few hours of complex soaking (Figure 9). Within the crystal, Ir−CO stretching (about 511 cm^{-1}) is covered by buffer and −S−S− stretching modes. Nevertheless, the entrance into the crystal of the Ir complex is well apparent from the additional low frequency bands (around 300 cm^{-1}), observed during the first hours of soaking. Initially, multiple Ir−Cl stretching bands are observed. This finding indicates the persistence of Cl in the Ir coordination sphere. These spectral features simplify in a broad band around 312 cm^{-1}, after about 1 day, that remains stable.

Considering the 2100 cm^{-1} spectral region (CO stretching region, Figure 10) other interesting features emerge. In particular, in $Cs_2[IrCl_5CO]$ powder, we can observe just one signal at about 2060 cm^{-1}. After hours of $[IrCl_5CO]_2^-$ soaking into HEWL crystals, three new bands are observed: a 2076 cm^{-1} band and a shoulder at 2122 cm^{-1} and a very intense signal at 2173 cm^{-1} (Figure 10, 5 h). These features are persistent for days (data not shown).

The experiment in Figure 10 is different when compared to that shown in Figure 9. Indeed, in Figure 10, Raman spectra collected after opening and closure of the crystallization box, planned to follow the re-equilibration of the CO-related bands upon removal of free CO gas, were reported.

Upon opening the crystallization box, the sharp signal at 2173 cm^{-1} almost disappears (Figure 10, 1 day). Upon closing again the crystallization box, the pattern 2076−2122−2173 cm^{-1} regains intensity (Figure 10, 5−15 days). We tentatively assign the 2076 cm^{-1} Raman bands to a mixture of unbound compounds ($[IrCl_5CO]^{2-}$ and $[IrCl_4CO(H_2O)]^-$); the 2173 cm^{-1} signal is assigned to free CO trapped into protein crystal, whereas the transient band at 2122 cm^{-1} is tentatively assigned to the adduct formed with His15 $[IrCl_4CO(His)]$.

According to the overall Raman-crystallographic interpretation, we can draw a clear picture of protein−$[IrCl_4CO(H_2O)]^-$ interaction and of CO pathway in and out from the protein crystal:

(a) $[IrCl_4CO(H_2O)]^-$ entry from solution into the crystal.
(b) interaction with the protein and subsequent coordination to His15 side chain (Figure 1). This ligated form is stable for several days (Raman data not shown and Figure 1), as long as the CO release starts.
(c) CO release from the non-covalently bound Ir compounds (Figure 10, 1day) and subsequent release of these compounds;
(d) CO release from the covalently bound Ir-compounds, i.e. those linked to His15 (Figures 9 and 10, 37 days).

In order to analyze the HEWL ability to incorporate CO into the protein core, implicit ligand sampling[35] (ILS) free energy calculations of CO migration to the HEWL core were performed over the 50 ns MD simulation aforementioned. Our results show that the two lowest barriers to be crossed for CO to get inside of the protein are about 9 and 17 kcal/mol. Furthermore, no energetically favorable cavities for storing CO can be seen by the inspection of the ILS maps. These data suggest that, upon releasing from the CORM, the CO molecule cannot be trapped by the protein matrix/core in solution.

CONCLUSIONS

In this work, we have investigated the reactivity of $[IrCl_5CO]^{2-}$ with a model protein. Unambiguous evidence is provided for His15 as the primary anchoring site for the Ir derivative, thus suggesting that this maybe an operative mechanism for CORM−protein binding and CO release in proteins with exposed His residues. Interestingly, in the case of the HEWL−$[IrCl_5CO]^{2-}$ adduct, halogen bonding interactions[42] form between the ligand and the protein. This result provides a further support to the recent idea that halogen bonds may be capable of critically enhancing the binding affinity of small compounds for pharmacological targets.[43,44]

The results of this work demonstrate that the formation of macromolecular adducts between the CO-containing iridium compounds and proteins can be reached via either covalent or non-covalent interactions. This feature could be an advantage for its medical applications, since it could be used to tune the CO releasing rate. In fact, this type of complex is the best system for delivering the particular derivative at interest site. Covalent adduct assures the stability of the complex and could help to achieve slow release of CO molecules and then the release of the complex from the protein. Vice versa, the non-covalent interactions are more labile and could produce a faster CO release. These findings suggest that once formed, CO containing Ir molecule−protein adducts could remain in circulation even for a long time, while they slowly decay, as recently suggested for CORM-3.[17,18] In this process adducts can release CO in different amounts and at different times. Both, a quick and slow delivery of CO through the blood via protein adducts could become a useful strategy for therapeutic CO delivery in vivo.

ASSOCIATED CONTENT

Supporting Information

Figures S1 and S2 and Tables S1 and S2. This material is available free of charge via the Internet at http://pubs.acs.org.

AUTHOR INFORMATION

Corresponding Author

*Fax: +39081674090. E-mail: antonello.merlino@unina.it.

Author Contributions

The manuscript was written through contributions of all authors. All authors have given approval to the final version of the manuscript.

Notes

The authors declare no competing financial interest.

ACKNOWLEDGMENTS

D.A.E. acknowledges University of Buenos Aires and CONICET for financial support. The authors thank G. Sorrentino and M. Amendola for technical assistance and M. Marti for helpful discussions.

REFERENCES

(1) Motterlini, R.; Sawle, P.; Hammad, J.; Bains, S.; Alberto, R.; Foresti, R.; Green, C. J. *FASEB J.* **2005**, *19*, 284−6.
(2) Johnson, T. R.; Mann, B. E.; Clark, J. E.; Foresti, R.; Green, C. J.; Motterlini, R. *Angew. Chem., Int. Ed.* **2003**, *42*, 3722−9.
(3) Motterlini, R.; Clark, J. E.; Foresti, R.; Sarathchandra, P.; Mann, B. E.; Green, C. J. *Circ. Res.* **2002**, *90*, E17−24.
(4) Pizarro, M. D.; Rodriguez, J. V.; Mamprin, M. E.; Fuller, B. J.; Mann, B. E.; Motterlini, R.; Guibert, E. E. *Cryo-biology* **2009**, *58*, 248−55.
(5) Desmard, M.; Davidge, K. S.; Bouvet, O.; Morin, D.; Roux, D.; Foresti, R.; Ricard, J. D.; Denamur, E.; Poole, R. K.; Montravers, P.; Motterlini, R.; Boczkowski, J. *FASEB J.* **2009**, *23*, 1023−31.

(6) Bani-Hani, M. G.; Greenstein, D.; Mann, B. E.; Green, C. J.; Motterlini, R. *Pharmacol. Rep.* **2006**, *58* (Suppl), 132−44.
(7) Motterlini, R.; Haas, B.; Foresti, R. *Med. Gas Res.* **2012**, *2*, 28.
(8) Schallner, N.; Schwemmers, S.; Schwer, C. I.; Froehlich, C.; Stoll, P.; Humar, M.; Pahl, H. L.; Hoetzel, A.; Loop, T.; Goebel, U. *Eur. J. Pharmacol.* **2011**, *670*, 58−66.
(9) Wilson, J. L.; Jesse, H. E.; Hughes, B. M.; Lund, V.; Naylor, K.; Davidge, K. S.; Cook, G. M.; Mann, B. E.; Poole, R. K. *Antioxid. Redox Signal* **2013**, *19*, 497−509.
(10) Schwer, C. I.; Mutschler, M.; Stoll, P.; Goebel, U.; Humar, M.; Hoetzel, A.; Schmidt, R. *Mol. Pharmacol.* **2010**, *77*, 660−9.
(11) Mahan, V. L. *Med. Gas Res.* **2012**, *2*, 32.
(12) Atkin, J.; Williams, S.; Sawle, P.; Motterlini, R.; Lynam, J. M.; Fairlamb, I. J. *Dalton Trans.* **2009**, *19*, 3653−6.
(13) Rudolf, P.; Kanal, F.; Gehrig, D.; Niesel, J.; Brixner, T.; Schatzschneider, U.; Nuernberger, P. *J. Phys. Chem. Lett.* **2013**, *4*, 596−602.
(14) Bikiel, D. E.; Gonzalez Solveyra, E.; Di Salvo, F.; Milagre, H. M.; Eberlin, M. N.; Correa, R. S.; Ellena, J.; Estrin, D. A.; Doctorovic, F. *Inorg. Chem.* **2011**, *50*, 2334−45.
(15) Boczkowski, J.; Poderoso, J. J.; Motterlini, R. *Trends Biochem. Sci.* **2006**, *31*, 614−21.
(16) Herrick, R. S.; Ziegler, C. J.; Leeper, T. C. *J. Organomet. Chem.* **2014**, *751*, 90−110.
(17) Santos-Silva, T.; Mukhopadhyay, A.; Seixas, J. D.; Bernardes, G. J.; Romao, C. C.; Romao, M. J. *J. Am. Chem. Soc.* **2011**, *133*, 1192−5.
(18) Santos-Silva, T.; Mukhopadhyay, A.; Seixas, J. D.; Bernardes, G. J.; Romao, C. C.; Romao, M. J. *Curr. Med. Chem.* **2011**, *18*, 3361−6.
(19) Santos, M. F.A.; Seixas, J. D.; Coelho, A.; Mukhopadhyay, A.; Reis, P. M.; Romao, M. J.; Romao, C. C.; Santos-Silva, T. *J. Inorg. Biochem.* **2012**, *117*, 285−291.
(20) Seixas, J. D.; Mukhopadhyay, A.; Santos-Silva, T.; Otterbein, L. E.; Gallo, D. J.; Rodrigues, S. S.; Guerreiro, B. H.; Goncalves, A. M. L.; Penacho, N.; Marques, A. R.; Coelho, A. C.; Reis, P. M.; Romao, M. J.; Romao, C. C. *Dalton. Trans.* **2013**, *42*, 5985−98.
(21) Russo Krauss, I.; Sica, F.; Mattia, C. A.; Merlino, A. *Int. J. Mol. Sci.* **2012**, *13*, 3782−800.
(22) Minor, W.; Cymborowski, M.; Otwinowski, Z.; Chruszcz, M. *Acta Cryst. D* **2006**, *62*, 859−66.
(23) Brunger, T.; Adams, P. D.; Clore, G. M.; DeLano, W. L.; Gros, P.; Grosse-Kunstleve, R. W.; Jiang, J. S.; Kuszewski, J.; Nilges, M.; Pannu, N. S.; Read, R. J.; Rice, L. M.; Simonson, T.; Warren, G. L. *Acta Cryst. D* **1998**, *54*, 905−21.
(24) Vaney, M. C.; Maignan, S.; Ries-Kautt, M.; Ducriux, A. *Acta Cryst. D* **1996**, *52*, 505−17.
(25) Jones, T. A.; Zou, J. Y.; Cowan, S. W.; Kjeldgaar, M. *Acta Cryst. A* **1991**, *47*, 110−119.
(26) Laskowski, R. A.; MacArthur, M. W.; Moss, D. S.; Thornton, J. M. *J. Appl. Crystallogr.* **1993**, *26*, 283−291.
(27) Hooft, R. W.; Sander, C.; Vriend, G. *Comput. Appl. Biosci.* **1997**, *13*, 425−430.
(28) Vergara, A.; Merlino, A.; Pizzo, E.; D'Alessio, G.; Mazzarella, L. *Acta Cryst. D* **2008**, *64*, 167−71.
(29) Jorgensen, W. L.; Chandrasekhar, J.; Madura, J. D.; Impey, R. W.; Klein, M. L. *J. Chem. Phys.* **1983**, *79*, 926.
(30) Luty, B. A.; Tironi, I. G. *Chem. Phys.* **1995**, *103*, 3014.
(31) Case, D. A.; Darden, T. A.; Cheatham, T. E.; Simmerling, C. L.; Wang, J.; Duke, R. E.; Luo, R.; Crowley, M.; Walker, R. C.; Zhang, W.; Merz, K. M.; Wang, B.; Hayik, S. ; Roitberg, A.; Seabra, G.; Kolossvry, I.; Wong, K. F.; Paesani, F.; Vanicek, J.; Wu, X.; Brozell, S. R.; Steinbrecher, T.; Gohlke, H.; Yang, L.; Tan, C.; Mongan, J. ; Hornak, V.; Cui, G.; Mathews, D. H.; Seetin, M. G.; Sagui, C.; Babin, V.; Kollman, P. A. *Amber 10*. University of California: San Francisco, 2008.
(32) Wang, J.; Wolf, R. M.; Caldwell, J. W.; Kollman, P. A.; Case, D. A. *J. Comput. Chem.* **2004**, *25*, 1157−1174.
(33) Rulisek, L.; Ryde, U. *J. Phys. Chem. B* **2006**, *110*, 11511−11518.
(34) Bayly, C. I.; Cieplak, P.; Cornell, W.; Kollman, P. A. *J. Phys. Chem. B* **1993**, *97*, 10269−10280.
(35) Cohen, J.; Arkhipov, A.; Braun, R.; Schulten, K. *Biophys. J.* **2006**, *91*, 1844−57.
(36) Forti, F.; Boechi, L.; Estrin, D. A.; Marti, M. A. *J. Comput. Chem.* **2011**, *32*, 2219−31.
(37) Boechi, L.; Marti, M. A.; Vergara, A.; Sica, F.; Mazzarella, L.; Estrin, D. A.; Merlino, A. *IUBMB Life* **2011**, *63*, 175−82.
(38) Policar, C.; Waern, J. B.; Plamont, M.-A.; Clede, S.; Mayer, C.; Prazeres, R.; Ortega, J.-M.; Vessiéres, A.; Dazzi, A. *Angew. Chem., Int. Ed.* **2011**, *123*, 890−894.
(39) Clede, S.; Lambert, F.; Sandt, C.; Gueroui, Z.; Refregiers, M.; Plamont, M.-A.; Dumas, P.; Vessiéres, A.; Policar, C. *Chem. Commun.* **2012**, *48*, 7729−7731.
(40) Kong, K. V.; Lam, Z.; Lau, W. K. O.; Leong, W. K.; Olivo, M. *J. Am. Chem. Soc.* **2013**, *135*, 18028−18031.
(41) Meister, K.; Niesel, J.; Schatzschneider, U.; Metzler-Nolte, N.; Schmidt, D. A.; Havenith, M. *Angew. Chem., Int. Ed.* **2010**, *49*, 3310−3312.
(42) Metrangolo, P.; Resnati, G. *Chemistry* **2001**, *7*, 2511−9.
(43) Metrangolo, P.; Neukirch, H.; Pilati, T.; Resnati, G. *Acc. Chem. Res.* **2005**, *38*, 386−95.
(44) Cavallo, G.; Metrangolo, P.; Pilati, T.; Resnati, G.; Sansotera, M.; Terraneo, G. *Chem. Soc. Rev.* **2011**, *39*, 3772−83.